Silibinin Inhibits Tumor Growth in a Murine Orthotopic Hepatocarcinoma Model and Activates the TRAIL Apoptotic Signaling Pathway

SOUAD BOUSSEROUEL[1], GAETAN BOUR[2], HENRIETTE KAUNTZ[1], FRANCINE GOSSÉ[1], JACQUES MARESCAUX[2] and FRANCIS RAUL[1]

[1]*Laboratory of Nutritional Cancer Prevention, Faculty of Medicine; University of Strasbourg, France;*
[2]*Research Institute against Digestive Cancer – European Institute of TeleSurgery, Strasbourg, France*

Abstract. *Aim: The present study investigated the molecular mechanism of silibinin-induced antitumoral effects in hepatocarcinoma Hep-55.1C cells in vitro and in a hepatocarcinoma model in mice. Materials and Methods: Cell death was analyzed by flow cytometry. The genetic expression of apoptotic and inflammatory biomarkers was assessed by quantitative Reverse Transcriptase Polymerase Chain Reaction (qRT-PCR). Orthotopic grafting of Hep-55.1C cells into the liver of C57BL/6J mice was performed, and tumor growth was followed by micro-computed imaging. Results: Silibinin activated the extrinsic apoptotic pathway in Hep55.1C cells, as attested by the up-regulation of TNF-related apoptosis-inducing ligand (TRAIL) and TRAIL Death receptor 5 (DR5) transcripts, and by the activation of caspase-3 and -8. After grafting of Hep-55.1C cells into mouse liver, the oral administration of silibinin at 700 mg/kg body weight for four weeks caused a significant reduction of tumor growth, associated with the down-regulation of inflammatory components [matrix metalloproteinase -7 and -9, (MMP-7, MMP-9), Interleukin-1 beta (IL1β)], the up-regulation of apoptotic mediators (TRAIL, DR5), and caspase-3 activation. Conclusion: Silibinin treatment exerted important anticarcinogenic effects, including the activation of TRAIL death receptor apoptotic signaling pathway in Hep-55.1C hepatocarcinoma cells, both in vitro and in hepatocarcinoma grafts in mice.*

This article is freely accessible online.

Correspondence to: Dr. Francis Raul, Laboratory of Nutritional Cancer Prevention, IRCAD, 1, Place de l'hôpital, 67091 Strasbourg-Cedex, France. Tel: +33 388119023, Fax: +33388119097. e-mail: francis.raul@ircad.u-strasbg.fr

Key Words: Liver cancer, inflammation, apoptosis, caspases, TRAIL, death receptor.

Hepatocellular carcinoma (HCC) ranks fifth in frequency among common human solid tumors and is the third leading cause of cancer-related death (1). The majority of HCC cases occur in Asia and Sub-Saharan Africa, but in recent years, HCC incidence has been increasing in Western Europe and the United States (2). Liver transplantation and surgical resection are considered as potential curative treatments for HCC. However these procedures are not relevant to HCC patients with concurrent liver cirrhosis, or metastatic spreading (3), and most HCC patients experience liver cancer recurrence after resection (4). Despite the use of several chemotherapeutic drugs in patients with HCC (5, 6), outcomes have not been promising for those with disease at advanced stages due to drug resistance and toxicity (7-9). Therefore, the search for additional drugs exhibiting no systemic toxicity should be widened in order to evaluate their potential growth-inhibitory effects in HCC. In this regard, traditional medicines and several phytochemical agents have been shown to be active towards human HCC cells (10, 11).

The flavonolignan silibinin, the major biologically active compound of milk thistle, has traditionally been used for the treatment of liver diseases in the form of milk thistle extract (12). Studies conducted by our group and others have revealed that in addition to its hepatoprotective effects, silibinin also exhibits strong anticancer efficacy towards various human cancer cell lines and also in several animal cancer models of various origin: prostate, bladder, skin, lung, colon *etc*. (13-16). We have reported that silibinin induces apoptosis in human colon adenocarcinoma and the derived metastatic cells partly through an activation of the TNF-related apoptosis-inducing ligand (TRAIL) death receptor pathway (16). In addition, we recently showed that intragastric feeding of silibinin to rats developing pre-neoplastic colonic lesions, reduced the number of these lesions by two-fold, inhibited the expression of pro-inflammatory mediators, and activated pro-apoptotic

processes (17). The present study aimed to determine whether silibinin activated similar mechanisms in Hep-55.1C hepatocarcinoma cells and in an orthotopic murine liver tumor model.

Considering the high lethality of liver cancer, it is necessary to gain further insight in our understanding of the disease and to develop new treatment strategies. For this purpose, several animal models exist, especially mouse models, including orthotopic graft models (18). The orthotopic implantation of HCC cells into the liver mimics better the cell environment, than does subcutaneous implantation. Tumor evolution is however more difficult to study, and on this respect we have reported methods to study tumor evolution non-invasively by micro-computed tomography (CT) follow-up (19, 20). By using syngeneic cells grafted orthotopically in immune-competent mice, the host immune system is active and closely represents the real tumoral microenvironment. Murine HCC cells transplanted into the liver of C57BL/6J mice produce syngeneic orthotopic grafts that histologically reproduce the parental tumors from which they are derived.

Materials and Methods

Cell culture and treatment. Hep55.1C cells (Cell Lines Service, Eppelheim, Germany) were cultured in 75 cm^2 Falcon flasks in Dulbecco's modified Eagle's medium (DMEM) containing 25 mM glucose and supplemented with 10% heat-inactivated (56˚C) horse serum, 100 U/ml penicillin, 100 μg/ml streptomycin and 1% non-essential amino acids (Invitrogen Corp., France). Cells were kept at 37˚C in a humidified atmosphere with 5% CO_2 and were subcultured after trypsinization (0.5% trypsin/2.6 mM ethylenediamine tetra-acetic acid). For all experiments, cells were seeded at 1×10^6 cells in culture dishes (10 cm internal diameter), and the culture medium was DMEM supplemented with 3% heat-inactivated horse serum and 100 U/ml penicillin, 100 μg/ml streptomycin, and 1% non-essential amino acids. Transferrin (5 μg/ml), selenium (5 ng/ml) and insulin (10 μg/ml) were added to compensate for the lower serum concentration. The culture medium was replaced every 48 h. Cells were exposed to silibinin (Sigma-Aldrich, Steinheim, Germany) 24 h after seeding. Silibinin was dissolved in dimethylsulfoxide (DMSO; Sigma-Aldrich) and used at a final concentration of 150 μg/ml. The final concentration of DMSO in culture media did not exceed 0.1%.

Cell death analysis by flow cytometry. Cell death was analyzed by flow cytometry as follows: 1×10^6 Hep55.1C cells were seeded in culture dishes and harvested by trypsinization at different time points (24, 48 and 72 h) after initial treatment with silibinin (150 μg/ml). Cells were centrifuged and fixed in 70% ethanol at –20˚C for at least 30 min, washed twice in phosphate-buffered saline (PBS) and re-suspended in 200 μl PBS containing 0.25 μg/ml RNase A and 0.1 mg/ml propidium iodide (Sigma-Aldrich). After incubation in the dark at 37˚C for 30 min, the fluorescence of 10,000 cells was analyzed by flow cytometry using CellQuest software (FACScan, BD Biosciences, Belgium).

Measurement of caspase-3 and caspase-8 activities. Caspase activity was measured by colorimetric assay kits (Sigma-Aldrich) according to the manufacturer's instructions. Briefly, 20 μl of cell lysate or tissue lysate were added to a buffer containing a *p*-nitroaniline (pNA)-conjugated substrate for caspase-3 (Ac-DEVD-pNA) or -8 (Ac-IETD-pNA) to a total of 100 μl reaction volume. Incubation was carried out at 37˚C. The concentration of the released pNA was calculated from the absorbance values at 405 nm and the calibration curve of defined pNA solutions. Results were adjusted according to the protein content, and activities are expressed as the fold-increase of the caspase activity of the untreated cells. For tissue, activities were expressed as fold-increase of the caspase activity of the tumor tissue over that of the paired adjacent normal liver tissue.

Orthotopic graft of Hep55.1C cells in C57BL/6J mice. Male C57BL/6J mice were purchased from Janvier breeding facilities (St Genest, France) and housed under standard conditions. All animal experiments were performed in accordance with the institutional guidelines of the French Ethical Committee (authorization no. A67-480, French Ministry of Agriculture). For orthotopic tumor graft, 8-week-old C57BL/6J mice were anesthetized by inhalation of isoflurane (Forene, Abbott, Rungis, France). Orthotopic grafting was performed as described previously (20). Briefly, 2×10^6 Hep-55.1C cells resuspended in 30 μl of PBS (Sigma-Aldrich) were injected into the lateral lobe of the left liver after midline laparotomy. Following hemostasis, the abdomen was closed in two layers. Tumor evolution was followed up by microCT imaging.

MicroCT liver imaging. MicroCT images were obtained on a micro CAT II scanner (Imtek Inc, Knoxville, TN) at 80 kVp X-ray voltage and 500 μA anode current under general gaseous anesthesia with isoflurane (Abbott). Respiratory-gated images were acquired with a resolution of 119 μm leading to a scanned volume of 6.1×6.1×6.1 cm. Based on previous experiments, four hours before the first imaging, animals were injected intraperitoneally with 6 μl/g Exitron Nano 6000 (Miltenyi, France) liver contrast agent. This nanoparticle-based contrast agent is taken up by macrophages (Küppfer cells) and remains for several weeks in healthy liver, but is not taken up by tumor cells. Hep-55.1C tumors appear as hypodense black areas inside the white contrasted normal liver parenchyma. The presence of a tumor was assessed by microCT scan one week after tumor grafting. Images were analyzed with VR Render software and 3D reconstruction and volume determination was performed with the 3DVPM software developed at Research Institute against Digestive Cancer (IRCAD) (21).

Experimental design and treatment. One week after the tumor graft, the mice were randomized into two groups (n=6 per group). The control group received daily gavage (0.3 ml) on 5 days/week for 4 weeks of a vehicle solution (0.5% carboxymethyl cellulose and 0.025% Tween20). The other group received silibinin by gavage at a daily dose of 700 mg/kg body weight on 5 days/week for 4 weeks, in vehicle solution. In both treated and control groups, tumor volumes were recorded by microCT imaging. At the end of the experimental period, after euthanasia, liver tumors were measured with a caliper, isolated, and weighed. The evolution of tumor volume was calculated by normalizing the volume calculated at each time-point from microCT scan images after 3D reconstruction of the tumor with the tumor volume calculated before the first treatment. Tumor volume at autopsy was determined using the semi-ellipsoid volume formula: $\pi/6$ (length×width×height).

Real-time quantitative reverse-transcriptase polymerase chain reaction (qRT-PCR) analysis. Total RNA was isolated from Hep55.1C cells in culture, and from HCC tumor tissue and adjacent normal liver tissue in mice using RNeasy Plus Mini Kit (Qiagen, Austin, TX, USA). A High Capacity cDNA Reverse Transcription Kit (Applied Biosystems, Foster City, CA) was used for cDNA synthesis as recommended by the supplier. qRT-PCR was performed by using ABI TaqMan gene expression assays for matrix metalloproteinase 7 and 9 (MMP-7 assay ID: Mm00487724_m1; MMP-9 assay ID: Mm00442991_m1), Interleukin-1 beta (IL1β assay ID: Mm01336189_m1), and Death receptor 5 (DR5 assay ID: Mm00457866_m1), TNF-related apoptosis-inducing ligand (TRAIL assay ID: Mm01283606_m1), and Interferon gamma (*IFN-γ* assay ID: Mm01168134_m1), according to the manufacturer's instructions. All samples were run in triplicate in a 25 μl reaction volume. Quantitative real-time RT-PCR was performed using TaqMan Universal PCR Master Mix (Applied Biosystems) and an ABI Prism 7500 Sequence Detection System (Applied Biosystems) in triplicate wells. The data were analyzed using a comparative threshold cycle (CT) method. CT values were calculated using 7500 SDS software (Applied Biosystems). For each sample, expressions of genes were normalized with the mRNA expression of the mouse control gene *β-actin* (part no. 4352933E) and the fold difference between treated and non-treated Hep-55.1C cells and between tumor tissue and paired adjacent normal liver tissue calculated using the $2^{-\Delta\Delta Ct}$ method (22).

Statistical analysis. Data are reported as the mean±SE. Statistical differences between control and treated groups were evaluated using the Student's *t*-test or the Student–Neuman–Keuls multiple comparison test. Differences between groups are considered significant at $p<0.05$.

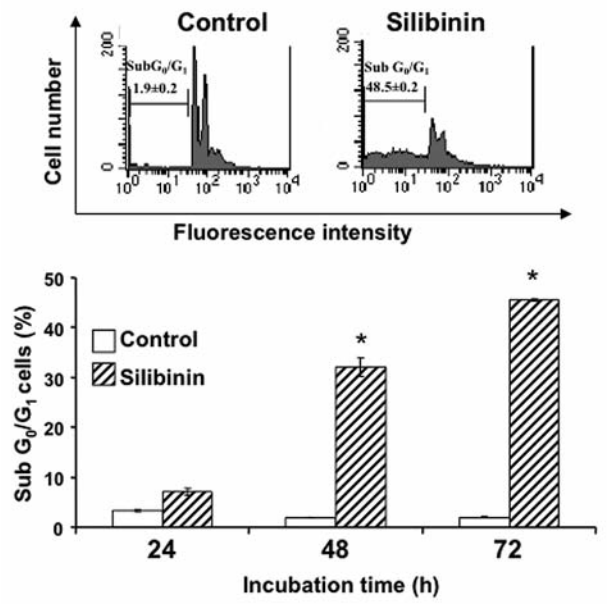

Figure 1. *Effects of silibinin on hepatocarcinoma cell death. Hep-55.1C cells were treated with DMSO 0.1% with/without silibinin (150 μg/ml) for 24, 48 or 72 h. At each time point, Hep-55.1C cells were harvested and stained with propidium iodide for the measurement of hypodiploid bodies and analyzed by flow cytometry as detailed in the Materials and Methods. The upper panel shows representative Fluorescence-activated cell sorting (FACS) histograms after 72 h of treatment. The percentage of silibinin-treated cells in the subG_0/G_1 region is indicated. In the lower panel, data are the mean value±SE of three separate experiments. *p<0.01 for silibinin treatment versus non-treated control.*

Results

Cell death induction by silibinin. After induction of cell death, DNA is degraded, leading to a DNA content lower than 2n per cell. These cells are detected after propidium iodide labeling by flow cytometric analysis in the sub-G_0/G_1 region (23). We measured the proportion of hypodiploid cells (sub-G_0/G_1 population) 24, 48 and 72 h after silibinin treatment. Figure 1 shows that the sub-G_0/G_1 population of Hep-55.1C cells increased progressively with time after silibinin treatment. The percentage of hypodiploid cells rose from 9% (24 h) to 33% (48 h) and to 45% (72 h).

Silibinin activates the extrinsic apoptotic pathway. HCCs show resistance to death receptor-mediated apoptosis because the majority of HCCs exhibit one or more alterations in the TRAIL pathway signaling (24). The TRAIL death receptor DR5 triggers the extrinsic apoptotic pathway when activated (25). Treatment of Hep-55.1C cells with silibinin significantly increased the number of *DR5* and *TRAIL* transcripts compared to untreated cells (Figure 2A and 2B). The enhanced expression of TRAIL and DR5 transcripts is not in itself a proof for the activation of the extrinsic apoptotic pathway, which implies the activation of caspase-8 by DR5. These caspases may then activate the effector caspase-3, leading to cell death. Therefore we assessed the activities of caspase-3 and caspase-8 by measuring the colorimetric reaction product resulting from the cleavage of their respective specific substrates, Ac-DEVD-pNA for caspase-3, and LEHD-pNA for caspase-8. We observed that caspase-3 and caspase-8 were both activated in Hep-55.1C cells treated with silibinin (Figure 3A and 3B).

Silibinin treatment inhibits mice Hep-55.1C liver tumor growth. Based on our data showing the involvement of TRAIL apoptotic pathway in Hep-55.1C cell death triggered by silibinin, we examined the *in vivo* efficacy of silibinin in orthotopic grafts of Hep-55.1C cells in the liver of C57BL/6J mice. The growth of liver tumors was followed by microCT imaging using a micro CAT II scanner (Figure 4A). The time-dependent growth of HCC tumors was evidenced by an innovative method of 3D reconstruction derived from microCT scans of livers and tumors, allowing the measurement of tumor volume (Figure 4B). The administration of silibinin (700 mg/kg body weight) by oral gavage on 5 days/week for 4 weeks caused a marked time-dependent inhibition in tumor growth in comparison to the

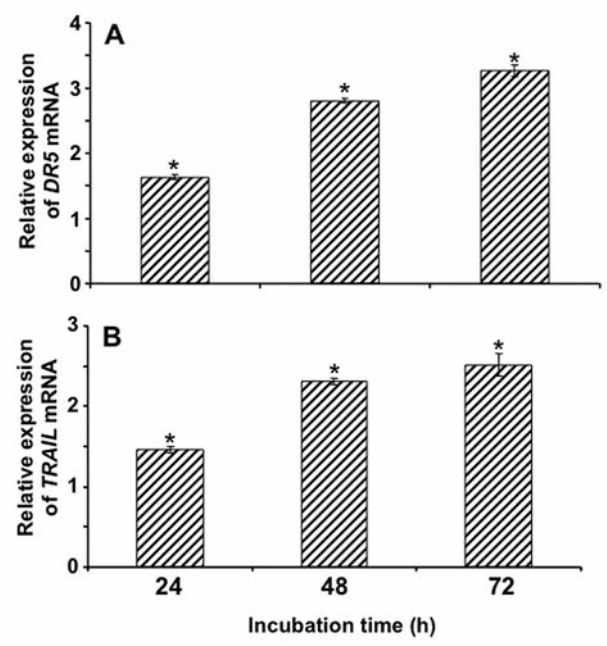

Figure 2. *Changes in the mRNA expression level of TNF-related apoptosis-inducing ligand (TRAIL) death receptor DR5 (A) and in the mRNA expression of TRAIL (B) after silibinin treatment. Hep-55.1C cells were treated with DMSO 0.1% with/without silibinin (150 μg/ml) for 24, 48 and 72 h. Total RNA was isolated and qRT-PCR was performed as detailed in the Materials and Methods. Data are the mean value±SE of three separate experiments. *p<0.01 for silibinin treatment versus non-treated control.*

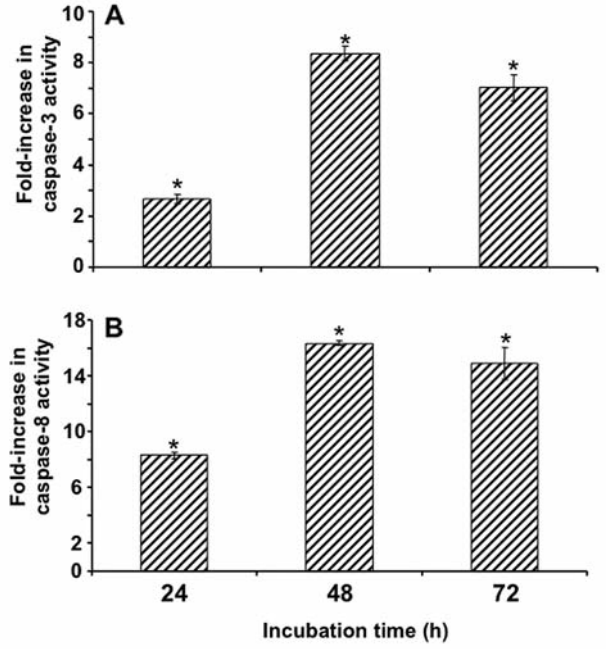

Figure 3. *Effects of silibinin on caspase-3 and caspase-8 activities. Cells were treated with DMSO 0.1% with/without silibinin (150 μg/ml) for 24, 48 and 72 h. Caspase activities were determined by colorimetric method using specific substrates as described in the Materials and Methods. Data are indicated as the fold increase of caspase-3 (A) and caspase-8 (B) activity in silibinin-treated Hep-55.1C cells over that of non-treated cells. Data are presented as the mean value±SE of three separate experiments. *p<0.05 for silibinin treatment versus non-treated control.*

tumors of vehicle-treated animals. Longitudinal imaging analysis also provided information on tumor volume change, confirming the efficacy of silibinin treatment (Figure 4B). A three-fold reduction of the relative tumor size was observed in animals receiving silibinin after two weeks of treatment when compared to the untreated group. At autopsy, a three-fold reduction of tumor weight and volume was also recorded (Figure 4C).

Silibinin treatment did not lead to any toxic effects since similar behavior, body weight and diet consumption were observed in control and silibinin-treated mice.

Inflammatory and apoptotic gene expression changes in liver tumors. In order to gain more insight into the mechanisms underlying the *in vivo* antitumor efficacy of silibinin, orthotopic tumors were analyzed by real-time quantitative RT-PCR for the differential expression of inflammatory (IL1β, MMP-7 and MMP-9) and innate immunity components (IFN-γ) (Figure 5). As shown in Figure 5A, tumors from silibinin-fed groups exhibited a significant ($p<0.01$) decrease in the expression of both matrix metalloproteinases studied (MMP-7 and MMP-9), when compared to untreated controls. It has been reported that transcription of the *MMP* genes is positively regulated by cytokines and growth factors such as interleukins (IL1β), suspected to be associated with HCC growth (26-28). Accordingly, we report here a significant up-regulation of both *IL1β* mRNA (more than 10-fold) in the liver tumor of controls compared to a healthy section of their liver. Silibinin treatment caused a significant ($p<0.01$) reduction of *IL1β* mRNA, to the level found in the healthy section of the liver (Figure 5B). We also found that the mRNA expression of *IFN-γ*, a biomarker of the innate immune system, was up-regulated by 25-fold in the liver tumor of silibinin-treated mice compared to the liver tumor of untreated controls (Figure 5B).

Since we observed that silibinin exerted strong apoptotic effects in Hep-55.1C cells through an activation of the TRAIL death receptor apoptotic pathway, we examined the effect of silibinin on the expression of *DR5* and *TRAIL* in liver tumors by quantitative RT-PCR analyses. The present data showed that silibinin treatment significantly ($p<0.01$) up-regulated both *DR5* and of *TRAIL* transcript expressions, (Figure 6A). As shown here in *in vitro* experiments with

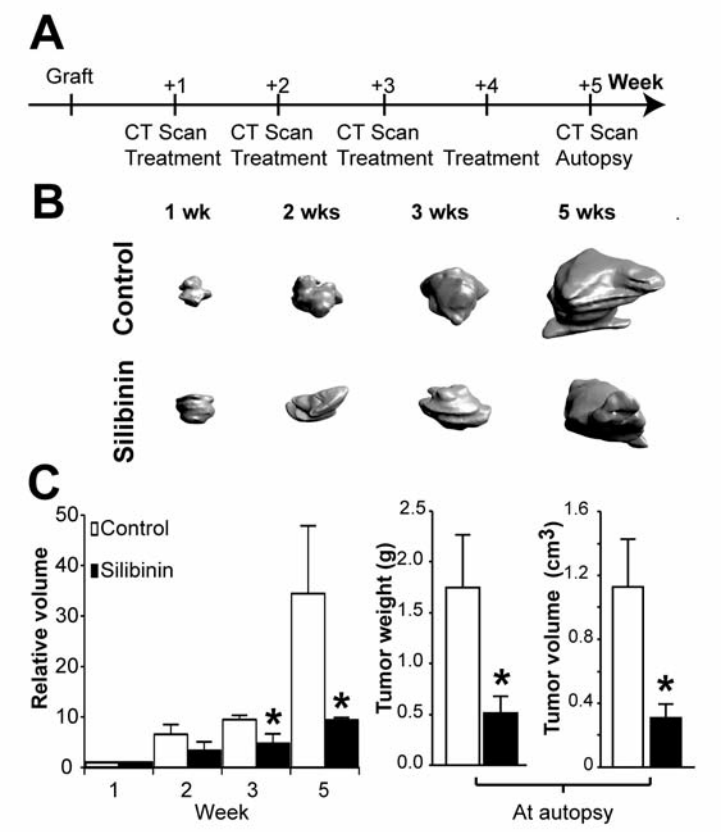

Figure 4. *Follow-up of tumor development after orthotopic grafting of hepatocarcinoma Hep-55.1C cells into the liver of mice. Tumor evolution was assessed by computed tomography (CT) with a microCT scanner followed by 3D reconstruction process, as described in the Materials and Methods. A: Experimental procedures. One week after tumor graft, the control group received daily gavage of the vehicle and by gavage the other group received silibinin at a daily dose of 700 mg/kg body weight, on 5 days a week for 4 weeks. B: Representative follow-up of liver tumor evolution in the same silibinin-treated mouse and a control mouse measured after 3D reconstruction of tumor volume from consecutive microCT scans. C: Tumor volumes were determined from the 3D reconstruction of the tumors and plotted as a ratio of the initial volume (relative volume). Tumor weight and tumor volume were also measured at autopsy. Data are presented as the mean±SE (6 mice per group). *p<0.05 for silibinin-treated mice versus controls.*

Hep-55.1C cells, the activation of the TRAIL death receptor pathway triggers the activation of caspase-3. Accordingly, we found a two-fold increase of caspase-3 activity in tumors of silibinin-treated mice when compared to liver tumors of control mice (Figure 6B).

Discussion

Hepatocellular carcinoma (HCC) is one of the most common types of cancer worldwide. HCC is resistant to conventional treatments (chemotherapy and radiotherapy) and this disease is therefore of very poor prognosis, urging for the development of more efficient therapeutic options. One of the key factors for successful use of therapeutic agents is the understanding of the mechanisms regulating drug delivery to the tumor, combined with the ability to provide a clear interpretation of their efficiency. To this aim, several imaging techniques have been developed in live animals, such as magnetic resonance imaging, CT, positron-emission tomography, and whole-body imaging using bioluminescence (29). Here, the growth of liver tumors was followed by micro CT imaging using a micro CAT II scanner. The evaluation of tumor growth was assessed using a 3D software developed at the IRCAD (21). Using this model, in a short-term study we showed that silibinin administered for four weeks, starting one week after orthotopic grafting of Hep-55.1C cells into liver of C57BL/6J mice, significantly reduced tumor growth and size. We hypothesized that these antitumor effects might be correlated to a silibinin-mediated activation of apoptotic cell death in liver tumors. The expression of death receptors DR4 and DR5 belonging to the family of TRAIL receptors are altered in patients with HCC, especially those at advanced stages (30).

In the present study, silibinin treatment induced an important up-regulation of pro-apoptotic TRAIL death receptor *DR5* and *TRAIL* gene expressions. These changes

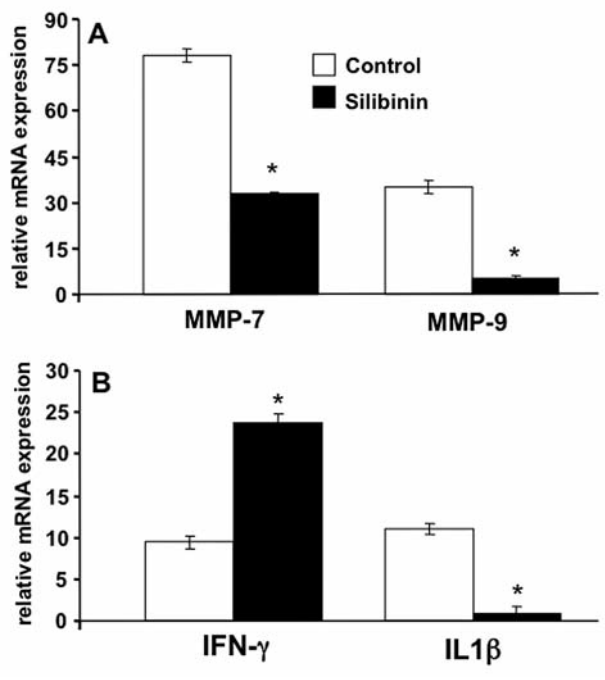

Figure 5. *Effect of silibinin on the genetic expression of pro-inflammatory cytokines, matrix metalloproteinases (MMPs) and biomarkers of the innate immune system. The levels of MMP-7 and MMP-9 (A), and of Interleukin-1 beta (IL1β) and Interferon gamma (IFN-γ) (B) transcripts were measured in tumor tissues and adjacent normal liver tissues by qRT-PCR as detailed in the Materials and Methods. Data are the mean value±SE (6 mice per group). *p<0.01 for silibinin-treated mice versus non-treated controls.*

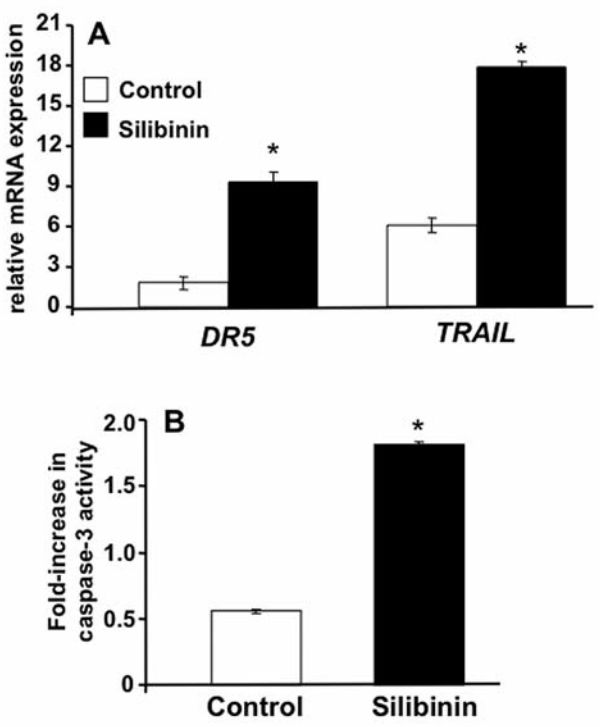

Figure 6. *Silibinin treatment activates apoptosis in liver tumors. A: The levels of TNF-related apoptosis-inducing ligand (TRAIL) and TRAIL death receptor (DR5) transcripts were measured by qRT-PCR as detailed in the Materials and Methods. Data are the mean value±SE (6 mice per group). *p<0.01 for silibinin-treated mice versus non-treated controls. B: Measurement of caspase-3 activity in tumors of silibinin-treated and of control mice. Caspase activity corresponds to the fold-increase in samples obtained from tumor relative to that of normal adjacent tissue. Data are the mean±SE. *p<0.01 for silibinin-treated mice versus non-treated controls.*

were associated with activation of caspase-3. These data were in accordance with our *in vitro* findings showing that silibinin-triggered activation of apoptosis in cultured Hep-55.1C cells was associated with the up-regulation of DR5 transcripts and the activation of caspases 3 and 8. These data show that in both *in vivo* and *in vitro* models, silibinin was able to activate the TRAIL death receptor apoptotic pathway.

The drug-resistance of liver tumors might also be related to various cells present in the tumor microenvironment, such as fibroblasts, endothelial cells, and immune cells (31). Fibroblasts, for example, provide growth signals by the secretion of transforming growth factor β, MMPs, and epidermal growth factor (32, 33). MMPs, which are mainly produced by nonmalignant stromal cells, are known to favor tumor growth, invasion, and metastasis (34), and drugs inactivating MMPs have been suggested to be useful in combination therapy with TRAIL (35). Our present data showed that expression of MMP-7 and, to a lesser extent MMP-9, was significantly ($p<0.01$) enhanced in the liver tumors and their expression levels were significantly ($p<0.01$) reduced by silibinin treatment. Furthermore, we observed that silibinin drastically reduces IL1β expression, which is known to induce the overexpression of MMPs (36). Thus, the reported inhibitory effects of silibinin on liver tumor growth may, also, be related to the down-regulation of these pro-inflammatory factors.

It has been suggested that tumor growth might be efficiently controlled by innate immunity components such as IFN-γ (37). A large number of studies have shown that IFN-γ production by T-cells is essential for tumor elimination (38). Here, we showed that silibinin treatment initiated a significant ($p<0.01$) up-regulation in the expression of IFN-γ in liver tumors. Furthermore, we found an inverse correlation between the expression of pro-inflammatory molecules (IL1β, MMP-7, MMP-9), and the expression of IFN-γ.

In conclusion, by using orthotopic syngeneic grafting of Hep-55.1C cells into C57BL/6J mouse liver and monitoring by microCT, we were able to show that the phytochemical

silibinin induced important anticarcinogenic and protective effects on the liver of mice. At a molecular level, these effects were associated with silibinin-induced inhibition of cellular pro-inflammatory factors, including IL1β, MMP-7, and MMP-9 expression, and these changes were associated with the increased expression of the host-defense mediator IFN-γ. We also demonstrated that silibinin-treatment triggered the activation of the TRAIL death receptor apoptotic signaling pathway in both Hep-55.1C hepatocarcinoma cells *in vitro* and in orthotopic tumor grafts of Hep-55.1C cells in mouse liver.

Acknowledgements

This study was supported by the Conseil Régional d'Alsace (France).

References

1 Ferlay J, Shin HR, Bray F, Forman D, Mathers C and Parkin DM: GLOBOCAN 2008 v1.2, Cancer Incidence and Mortality Worldwide. *In*: IARC CancerBase No. 10.Lyon, France: International Agency for Research on Cancer, 2010.

2 Seeff LB and Hoofnagle JH: Epidemiology of hepatocellular carcinoma in areas of low hepatitis B and hepatitis C endemicity. Oncogene *25*: 3771-3777, 2006.

3 Schafer DF and Sorrell MF: Hepatocellular carcinoma. Lancet *353*: 1253-1257, 1999.

4 Avila MA, Berasain C, Sangro B and Prieto J: New therapies for hepatocellular carcinoma. Oncogene *25*: 3866-3884. 2006.

5 Kojima S, Okuno M, Matsushima-Nishiwaki R, Friedman SL and Moriwaki H: Acyclic retinoid in the chemoprevention of hepatocellular carcinoma. Int J Oncol *24*: 797-805, 2004.

6 Yuan S, Zhang X, Lu L, Xu C, Yang W and Ding J: Anticancer activity of methoxymorpholinyl doxorubicin (P NU 152243) on human hepatocellular carcinoma. Anticancer Drugs *15*: 641-646, 2004.

7 Chun E and Lee KY: BCL-2 and BCL-xL are important for the induction of paclitaxel resistance in human hepatocellular carcinoma cells. Biochem Biophys Res Commun *315*: 771-779, 2004.

8 Chao Y, Chan WK, Birkhofer MJ, Hu OY, Wang SS, Huang YS, Liu M, Whang-Peng J, Chi KH, Lui WY and Lee SD: Phase II and pharmacokinetic study of paclitaxel therapy for unresectable hepatocellular carcinoma patients. Br J Cancer *78*: 34-39, 1998.

9 O'Reilly EM, Stuart KE, Sanz-Altamira PM, Schwartz GK, Steger CM, Raeburn L, Kemeny NE, Kelsen DP and Saltz LB: A phase II study of irinotecan in patients with advanced hepatocellular carcinoma. Cancer *91*: 101-105, 2001

10 Su SJ, Chow NH, Kung ML, Hung TC and Chang KL: Effects of soy isoflavones on apoptosis induction and G_2-M arrest in human hepatoma cells involvement of caspase-3 activation, BCL-2 and BCL- down-regulation, and CDC2 kinase activity. Nutr Cancer *45*: 113-123, 2003.

11 Kao ST, Yeh CC, Hsieh CC, Yang MD, Lee MR, Liu HS and Lin JG: The Chinese medicine Bu-Zhong-Yi-Qi-Tang inhibited proliferation of hepatoma cell lines by inducing apoptosis via G0/G1 arrest. Life Sci *69*: 1485-1496, 2001.

12 Luper S: A review of plants used in the treatment of liver disease: part 1. Altern Med Rev *3*: 410-421, 1998.

13 Deep G and Agarwal R: Chemopreventive efficacy of silymarin in skin and prostate cancer. Integr Cancer Ther *6*: 130-145, 2007.

14 Cheung CW, Taylor PJ, Kirkpatrick CM, Vesey DA, Gobe GC, Winterford C, Nicol DL and Johnson DW: Therapeutic value of orally administered silibinin in renal cell carcinoma: manipulation of insulin-like growth factor binding protein-3 levels. BJU Int *100*: 438-444, 2007.

15 Singh RP, Deep G, Chittezhath M, Kaur M, Dwyer-Nield LD, Malkinson AM and Agarwal R: Effect of silibinin on the growth and progression of primary lung tumors in mice. J Natl Cancer Inst *98*: 846-855, 2006.

16 Kauntz H, Bousserouel S, Gossé F and Raul F: Silibinin triggers apoptotic signaling pathways and autophagic survival response in human colon adenocarcinoma cells and their derived metastatic cells. Apoptosis *16*: 1042-1053, 2011.

17 Kauntz H, Bousserouel S, Gossé F, Marescaux J and Raul F: Silibinin, a natural flavonoid, modulates the early expression of chemopreventive biomarkers in a preclinical model of colon carcinogenesis. Int J Oncol in press, 2012.

18 Leenders MWH, Nijkamp MW and Borel Rinkes IHM: Mouse models in liver cancer research: A review of current literature. World J Gastroenterol *14*: 6915-6923, 2008.

19 Raul F, Gossé F, Osswald AB, Bouhadjar M, Foltzer-Jourdainne C, Marescaux J and Soler L: Follow-up of tumor development in the colon of living rats and implications for chemoprevention trials: Assessment of aspirin-difluoromethylornithine combination. Int J Oncol *31*: 89-95, 2007.

20 Aprahamian M, Bour G, Akladios CY, Fylaktakidou K, Greferath R, Soler L, Marescaux J, Egly JM, Lehn JM and Nicolau C: Myo-InositolTrisPyroPhosphate treatment leads to HIF-1α suppression and eradication of early hepatoma tumors in rats. Chembiochem *12*: 777-83, 2011.

21 Soler L, Delingette H, Malandain G, Montagnat J, Ayache N, Koehl C, Dourthe O, Malassagne B, Smith M, Mutter D and Marescaux J: Fully automatic anatomical, pathological, and functional segmentation from CT scans for hepatic surgery. Comput Aided Surg *6*: 131-142, 2001.

22 Livak KJ and Schmittgen TD: Analysis of relative gene expression data using real-time quantitative PCR and the 2(–Delta Delta C(T)) method. Methods *25*: 402-408, 2001.

23 Riccardi C and Nicoletti I: Analysis of apoptosis by propidium iodide staining and flow cytometry. Nat Protoc *1*: 1458-1461, 2006.

24 Herr I, Schemmer P and Buchler MW: On the TRAIL to therapeutic intervention in liver disease. Hepatology *46*: 266-274, 2007.

25 Russo M, Mupo A, Spagnuolo C and Russo GL: Exploring death receptor pathways as selective targets in cancer therapy. Biochem Pharmacol *80*: 674-682, 2010.

26 Hirankarn N, Kimkong I, Kummee P, Tangkijvanich P and Poovorawan Y: Interleukin-1beta gene polymorphism associated with hepatocellular carcinoma in hepatitis B virus infection. World J Gastroenterol *12*: 776-779, 2006.

27 Yang Y, Luo C, Feng R and Bi S: The TNF-α, IL-1β and IL-39 polymorphisms and risk for hepatocellular carcinoma: a meta-analysis. J Cancer Res Clin Oncol *137*: 947-952, 2011.

28 Altadill A, Rodríguez M, González LO, Junquera S, Corte MD, González-Dieguez ML, Linares A, Barbón E, Fresno-Forcelledo M, Rodrigo L and Vizoso FJ: Liver expression of matrix metalloproteases and their inhibitors in hepatocellular carcinoma. Dig Liver Dis *41*: 740-748, 2009.

29 Willmann JK, van Bruggen N, Dinkelborg LM and Gambhir SS: Molecular imaging in drug development. Nat Rev Drug Discov *7*: 591-607, 2008.
30 Fabregat I. Dysregulation of apoptosis in hepatocellular carcinoma cells. World J Gastroenterol *15*: 513-520, 2009.
31 Mace TA, Yamane N, Cheng J, Hylander BL and Repasky EA: The potential of the tumor microenvironment to influence APO2L/TRAIL induced apoptosis. Immunol Invest *35*: 279-296, 2006.
32 Coussens LM and Werb Z: Inflammation and cancer. Nature *420*: 860-867, 2002.
33 Bhowmick NA, Neilson EG and Moses HL: Stromal fibroblasts in cancer initiation and progression. Nature *432*: 332-337. 2004.
34 Johansson N, Ahonen M and Kahari VM: Matrix metalloproteinases in tumor invasion. Cell Mol Life Sci *57*: 5-15, 2000.
35 Nyormoi O, Mills L and Bar-Eli M: An MMP-2/MMP-9 inhibitor, 5a, enhances apoptosis induced by ligands of the TNF receptor superfamily in cancer cells. Cell Death Differ *10*: 558-569, 2003.
36 Friedl P and Wolf K: Tumor-cell invasion and migration: Diversity and escape mechanisms. Nat Rev Cancer *3*: 362-374, 2003.
37 Jeong WI and Gao B: Innate immunity and alcoholic liver fibrosis. J Gastroenterol Hepatol *23(Suppl 1)*: S112-S118, 2008.
38 Blankenstein T: The role of tumor stroma in the interaction between tumor and immune system. Curr Opin Immunol *17*: 180-186, 2005.

Received April 18, 2012
Revised May 25, 2012
Accepted May 28, 2012